Journal of Optics B: Quantum and Semiclassical Optics

Complementary coherent state for measuring the *Q*-function: generation and properties

To cite this article: A T Avelar *et al* 2004 *J. Opt. B: Quantum Semiclass. Opt.* **6** 41

J. Opt. B: Quantum Semiclass. Opt. **6** (2004) 41–45 PII: S1464-4266(04)67182-5

Complementary coherent state for measuring the Q-function: generation and properties

A T Avelar[1,2], B Baseia[1] and N G de Almeida[1,3]

[1] Instituto de Física, Universidade Federal de Goiás, 74. 001-970, Goiânia (GO), Brazil
[2] Instituto de Física, Universidade de Brasília, 70. 919-970, Brasília (DF), Brazil
[3] Núcleo de Pesquisas em Física, Universidade Católica de Goiás, 74. 605-220, Goiânia (GO), Brazil

E-mail: nortongomes@ugc.br (N G de Almeida)

Received 5 August 2003, accepted for publication 3 October 2003
Published 20 October 2003
Online at stacks.iop.org/JOptB/6/41 (DOI: 10.1088/1464-4266/6/1/007)

Abstract
In a previous paper a proposal for measuring the Husimi Q-function based on the projection synthesis method (Barnett and Pegg 1996 *Phys. Rev. Lett.* **76** 4148) was presented. The scheme required the presence of an unavailable state, named the complementary coherent state. This paper shows how to generate this state in travelling waves and studies its properties.

Keywords: quantum state engineering, Husimi function, complementary coherent state

1. Introduction

An important issue of quantum optics in recent years is quantum state engineering (QSE), both for field [1–6] and atomic states [7]. Its relevance comes from the potential applications to advanced topics, such as teleportation [8], quantum computation [9], quantum communication [10], quantum cryptography [11], quantum lithography [12], decoherence of states [13], etc.

The field state being tailored may concern either stationary modes trapped inside a high-Q cavity [1–3] or travelling modes [4–6]. In the first case, QSE can be implemented either via resonant [1] or via nonresonant (dispersive) atom–field interaction [14]. In the second case, QSE may employ

(i) a coherent state travelling throughout a nonlinear medium [15],
(ii) an array of beam-splitters [4, 16],
(iii) an arrangement including beam-splitters and a nonlinear medium [17], etc.

In a recent paper, Barnett and Pegg [18] showed that an apparent 'exotic' state, then named the *reciprocal binomial state* (RBS), not available in laboratories, was crucial for their proposed experimental scheme determining the phase distribution of an arbitrary state of a running field. Later on [19], it was shown that the projection synthesis method proposed in [18] can also be used to determine the Husimi Q-function. In this case, another unknown state, then named the *complementary coherent state* (CCS), was crucial for such determination. The generation of the RBS has already been addressed in [20] for stationary modes and, as required in [18], for travelling modes [21]. Here we will consider the QSE concerning the generation of CCS for travelling modes, as required in [19].

This paper is organized as follows. In section 2 we introduce the CCS and propose its generation through a scheme developed by Dakna *et al* [16]. The fidelity of the generation process is calculated in section 3 via the Langevin method. For completeness, section 4 contains a resumed study of some nonclassical properties exhibited by the CCS, including its nonclassical depth. Section 5 contains comments and the conclusion.

2. Generation of CCS

The CCS was defined previously as [19]

$$|\mathrm{CCS}\rangle = \mathcal{N}\mathrm{e}^{-|\alpha|^2/2}\frac{2^{-N}}{\sqrt{N!}}\sum_{k=0}^{N}\sqrt{k!}\alpha^{*N-k}\mathrm{e}^{\mathrm{i}k\pi/2}|k\rangle \qquad (1)$$

where $\mathcal{N}$ is a normalization constant.

Table 1. The roots $\beta_k^* = |\beta_k| e^{-i\varphi_{\beta_k}}$ of the characteristic polynomial and the displacement parameters $\alpha_k^* = |\alpha_k| e^{-i\varphi_{\alpha_k}}$ are given for a CCS for $\alpha = 1.0$, $N = 5$ and $T = 0.957$. The probability of producing the state is 0.6%.

k	$\|\beta_k\|$	φ_{β_k}	$\|\alpha_k\|$	φ_{α_k}
1	0.626	−2.674	0.501	0.561
2	0.608	2.479	0.554	−1.692
3	0.631	−1.571	0.975	2.016
4	0.608	0.663	1.019	−2.016
5	0.626	−0.467	0.632	1.692
6			0.626	−0.467

As the CCS is a truncated state, we may employ the scheme introduced by Dakna *et al* [16]. For brevity the present application shows the relevant steps of [16] (and [21]), where the reader will find more details. In this scheme, a desired state $|\Psi\rangle$ composed of a finite number of Fock states $|n\rangle$ can be written as

$$|\Psi\rangle = \sum_{n=0}^{N} C_n |n\rangle = \frac{C_N}{\sqrt{N!}} \prod_{n=1}^{N} (\hat{a}^+ - \beta_n^*)|0\rangle = \frac{C_N}{\sqrt{N!}} \prod_{k=1}^{N} \hat{D}(\beta_k)\hat{a}^+ \hat{D}(\beta_k)|0\rangle, \tag{2}$$

where $\hat{D}(\beta_n)$ stands for the displacement operator and the β_n are the roots of the polynomial equation

$$\sum_{n=0}^{N} C_n \beta^n = 0. \tag{3}$$

According to the experimental set-up shown in figure 1 of [16] we have (assuming zero photons registered in all detectors) that the outcome state is

$$|\Psi\rangle \sim \prod_{k=1}^{N} D(\alpha_{k+1})\hat{a}^+ T^{\hat{n}} D(\alpha_k)|0\rangle, \tag{4}$$

where T is the transmittance of the beam-splitter and α_k are experimental parameters. After some algebra equations (2) and (4) can be connected. In this way, one shows that they become identical when $\alpha_1 = -\sum_{l=1}^{N} T^{-l}\alpha_{l+1}$ and $\alpha_k = T^{*N-k+1}(\beta_{k-1} - \beta_k)$ for $k = 2, 3, 4 \ldots, N$.

In the present case the coefficients C_n are given by those of the CCS. The roots $\beta_k^* = |\beta_k| e^{-i\varphi_{\beta_k}}$ of the characteristic polynomial in equation (3) and the displacement parameters $\alpha_k = |\alpha_k| e^{-i\varphi_{\alpha_k}}$ are shown in table 1, for $\alpha = 1.0$ and $N = 5$.

The probability of producing this state is $P_{|\text{CCS}\rangle} = 0.6\%$ for the beam-splitter transmittance $T = 0.957$, a value which optimizes the probability.

3. Fidelity of generation of CCS

Until now we have assumed all detectors and beam-splitters are ideal. Although very good beam-splitters are available by advanced technology, the same is not true for photodetectors in the optical domain. So, let us now take into account the quantum efficiency η at the photodetectors. For this purpose, we use the Langevin operator technique as introduced in [22] in order to obtain the fidelity to get the CCS.

Output operators accounting for the detection of a given field $\hat{\alpha}$ reaching the detectors are given by [22]

$$\hat{\alpha}_{\text{out}} = \sqrt{\eta}\hat{\alpha}_{\text{in}} + \hat{\mathsf{L}}_\alpha, \tag{5}$$

where η stands for the efficiency of the detector and $\hat{\mathsf{L}}_\alpha$, acting on the environment states, is the noise or Langevin operator associated with losses into the detectors placed in the path of modes $\hat{\alpha} = a, b$. We assume that the detectors couple neither different modes a, b nor the Langevin operators $\hat{\mathsf{L}}_\alpha$, so the following commutation relations are readily obtained from equation (5):

$$[\hat{\mathsf{L}}_\alpha, \hat{\mathsf{L}}_\alpha^\dagger] = 1 - \eta, \tag{6}$$

$$[\hat{\mathsf{L}}_\alpha, \hat{\mathsf{L}}_\beta^\dagger] = 0. \tag{7}$$

The ground-state expectation values for pairs of Langevin operators are

$$\langle \hat{\mathsf{L}}_\alpha \hat{\mathsf{L}}_\alpha^\dagger \rangle = 1 - \eta, \tag{8}$$

$$\langle \hat{\mathsf{L}}_\alpha \hat{\mathsf{L}}_\beta^\dagger \rangle = 0, \tag{9}$$

which are useful relations specially for optical frequencies, when the state of the environment can be very well approximated by the vacuum state, even for room temperature.

Let us now apply the scheme of [16] to the present case. For simplicity we will assume all detectors to have high efficiency ($\eta \gtrsim 0.9$). This assumption allows us to simplify the resulting expression by neglecting terms of order higher than $(1-\eta)^2$. When we do this, instead of $|\text{CCS}\rangle$, we find the state $|\Psi_{\text{FE}}\rangle$ describing the field plus environment, the latter being due to losses coming from the nonunit-efficiency detectors. We have

$$\begin{aligned}
|\Psi_{\text{FE}}\rangle \sim\ & R^N D(\alpha_{N+1})\hat{a}^+ T^{\hat{n}} D(\alpha_N)\hat{a}^+ T^{\hat{n}} \\
& \times D(\alpha_{N-1}) \cdots \hat{a}^+ T^{\hat{n}} D(\alpha_1)|0\rangle \hat{\mathsf{L}}_0^+ \\
& + R^{N-1} D(\alpha_{N+1})\hat{a}^+ T^{\hat{n}} D(\alpha_N)\hat{a}^+ T^{\hat{n}} \\
& \times D(\alpha_{N-1}) \cdots \hat{\mathsf{L}}_1^+ T^{\hat{n}} D(\alpha_1)|0\rangle \\
& + R^{N-1} D(\alpha_{N+1})\hat{a}^+ T^{\hat{n}} D(\alpha_N)\hat{\mathsf{L}}_{N-1}^+ T^{\hat{n}} \\
& \times D(\alpha_{N-1}) \cdots \hat{a}^+ T^{\hat{n}} D(\alpha_1)|0\rangle \\
& + R^{N-1} D(\alpha_{N+1})\hat{\mathsf{L}}_N^+ T^{\hat{n}} D(\alpha_N)\hat{a}^+ T^{\hat{n}} \\
& \times D(\alpha_{N-1}) \cdots \hat{a}^+ T^{\hat{n}} D(\alpha_1)|0\rangle,
\end{aligned} \tag{10}$$

where, for brevity, we have omitted the kets corresponding to the environment. Here R is the reflectance of the beam-splitter, $\hat{\mathsf{L}}_0^+ = \mathbf{1}$ is the identity operator and $\hat{\mathsf{L}}_k$, $k = 1, 2 \ldots, N$ stands for losses in the first, second ..., Nth detector. Although the $\hat{\mathsf{L}}_k$ commute with any system operator, we have maintained the order above to keep clear the set of possibilities for photoabsorption: the first term, which includes $\hat{\mathsf{L}}_0^+ = \mathbf{1}$, indicates the probability for nonabsorption; the second term, which includes $\hat{\mathsf{L}}_1^+$, indicates the probability for absorption in the first detector; and so on. Note that in the case of absorption at the kth detector, the annihilation operator a is replaced by the $\hat{\mathsf{L}}_k^+$ creation Langevin operator. Other possibilities such as absorption in more than one detector lead to a probability of order less than $(1-\eta)^2$, which will be neglected.

Next, we have to compute the fidelity[4], $F = \| \langle \Psi | \Psi_{\text{FE}} \rangle \|^2$, where $|\Psi\rangle$ is the ideal state given by equation (4), here

[4] The expression $F = |\langle \text{CCS}|\Psi_{\text{FE}}\rangle|^2$ stands for the usual abbreviation in the literature. Actually, this is equivalent to $\langle \Psi_{\text{CCS}}| \text{Tr}_E\, \hat{\varrho}_{\text{FE}} |\Psi_{\text{CCS}}\rangle$ where $\hat{\varrho}_{\text{FE}} = |\Psi_{\text{FE}}\rangle\langle\Psi_{\text{FE}}|$ and $\text{Tr}_E\, \hat{\varrho}_{\text{FE}}$ is the (*mixed*) smeared state, mentioned before.

corresponding to our CCS characterized by the parameters shown in table 1, and $|\Psi_{\rm FE}\rangle$ is the state given in equation (10). Assuming $\eta = 0.99$, 0.95, and 0.90 we find $F = 0.99$, 0.97, and 0.94, respectively. These high values of fidelity show that efficiencies around 0.9 lead to states whose degradation due to losses is not so dramatic.

Now, let us recall our initial purpose: using the CCS to determine the Husimi Q-function of an arbitrary field state. The foregoing results show that losses caused by the presence of nonideal phodetectors will transform our desired pure state (CCS) into a mixed state. As consequence, using a modified state, one will end up with modified properties measured upon the other state. So, a pertinent question is how to circumvent this problem. Fortunately, there is a solution to this problem provided by the inverse Bernouilli convolution (IBC), allowing one to *reconstruct* the desired pure state from the mixed state. Such a procedure has been implemented in the literature, in distinct scenarios [23, 24]. In this procedure a pure state, represented by the density operator $\varrho_{\rm p} = |\Psi\rangle\langle\Psi|$, can be reobtained from the smeared data contained in the mixed density operator. From the smeared data contained in the (mixed) density operator $\rho_{\rm out}(\mathbf{k}, \boldsymbol{\eta})$ one recovers the pure state as [24]

$$|\Psi\rangle\langle\Psi| = \frac{1}{p_0(\mathbf{1})} \sum_{k_1,\ldots,k_n} \{b_{o;k_1}(\eta_1^{-1}) \ldots b_{o;k_N}(\eta_N^{-1}) \times p_k(\boldsymbol{\eta})\rho_{\rm out}(\mathbf{k}, \boldsymbol{\eta})\}, \qquad (11)$$

where the functions $b_{o;k_i}$ are defined by

$$b_{l;m}(z) = \binom{m}{l} z^l (1-z)^{m-l}$$

and $\mathbf{k} = (k_1, \ldots, k_N)$ gives the number of counts obtained in the detectors.

At this point the following explanation is in order. Note that the IBC procedure is a theoretical correction, hence not able to experimentally purify the mixing introduced by nonideal detectors: the reconstruction is made upon computer data, not experimentally acting upon the running field states themselves. However, when applying a mixed output state in the measurement of a certain property of another field state one finally ends up with some measurement data, a set of numbers inside a computer and not a quantum state, these numbers being the final outcome of the entire procedure. Reconstruction of the initial data (the auxiliary pure state) yields the reconstruction of the final data (the measured property of another field state). So, it does not matter how this property has been obtained, whether theoretically or not.

4. Nonclassical properties of CCS

4.1. Photon number distribution

From equation (1) defining the CCS we find the statistical distribution $P_n = |C_n|^2$, where the C_n are the coefficients appearing in the expansion of the CCS in the Fock basis: $|{\rm CCS}\rangle = \sum_{n=0}^{N} C_n|n\rangle$. In this way we obtain from equation (1)

$$P_n = \mathcal{N}' n! |\alpha|^{2(N-n)} \qquad (12)$$

where $\mathcal{N}' = \left[\sum_{k=0}^{N} k!|\alpha|^{2(N-k)}\right]^{-1}$. Figure 1 shows the plots of the photon-number distribution P_n versus n, for the CCS specified by $N = 5$ and $\alpha = 1$. In this figure we note that P_n does not exhibit oscillations, hence the CCS shows no interference in the phase space; P_n increases (decreases) monotonically for $|\alpha| < 1.2$ ($|\alpha| > 2.2$), but exhibits a minimum for intermediate values of $|\alpha|$.

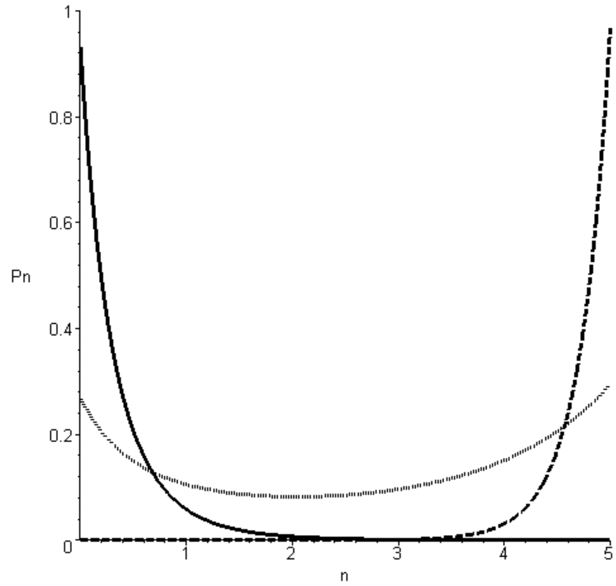

Figure 1. Plot of the photon-number distribution of the CCS, specified by $N = 5$ and $|\alpha| = 0.4$ (dashed curve), $|\alpha| = 1.4$ (dot curve), and $|\alpha| = 4.0$ (solid curve).

4.2. Sub-Poissonian statistics

Sub-Poissonian (SP) [25] and antibunching [26] constitute simultaneous effects for single-mode and stationary fields, as in the present case. So, the occurrence of one of them is sufficient to know about occurrence of the other. The SP effect is usually studied via the Mandel Q-parameter [25],

$$Q = (\Delta\hat{n}^2 - \langle\hat{n}\rangle)/\langle\hat{n}\rangle \qquad (13)$$

where $\Delta\hat{n}^2 = \langle\hat{n}^2\rangle - \langle\hat{n}\rangle^2$, with $\langle\hat{n}^k\rangle = \langle{\rm CCS}|\hat{n}^k|{\rm CCS}\rangle$, $k = 1, 2$. The SP effect results when $Q < 0$, namely $\Delta\hat{n}^2 < \langle\hat{n}\rangle$.

The substitution of equation (1) in equation (13) furnishes the value of the Mandel Q-parameter for the CCS. Figure 2 exhibits plots of the Mandel Q-parameter as a function of $|\alpha|$, for $N = 3$, 5, and 8. Note the occurrence of the SP effect for small values of $|\alpha|$. The interval of $|\alpha|$ for which $Q \sim -1$ increases when the Hilbert space dimension N grows.

4.3. Wigner function

The Wigner function describes the system completely and can be obtained from the $R(z, \tau)$ function [29],

$$R(z,\tau) = \frac{1}{\pi\tau} \int {\rm d}^2\alpha \exp\left(-\frac{1}{\tau}|z-\alpha|^2\right) P(\alpha) \qquad (14)$$

for $\tau = 1/2$. In equation (14) $P(\alpha)$ is the Glauber–Sudarshan quasi-probability function [27]. Negative values of the

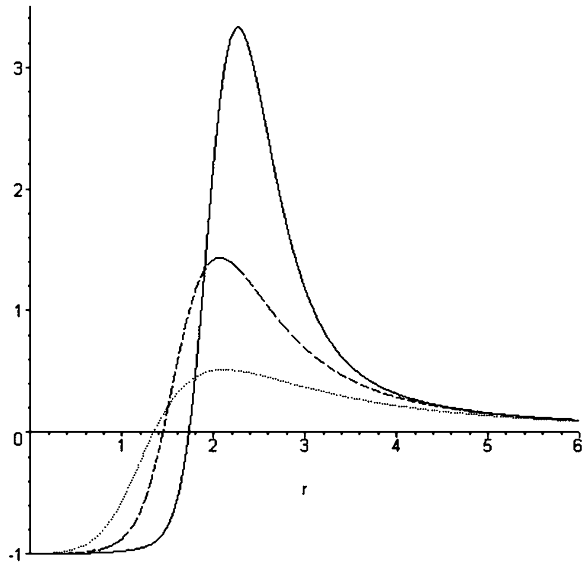

Figure 2. Plot of the Mandel Q-parameter for the CCS, as a function of $r = |\alpha|$ for the CCS specified by $N = 3$ (dotted curve), $N = 5$ (dashed curve), and $N = 8$ (solid curve).

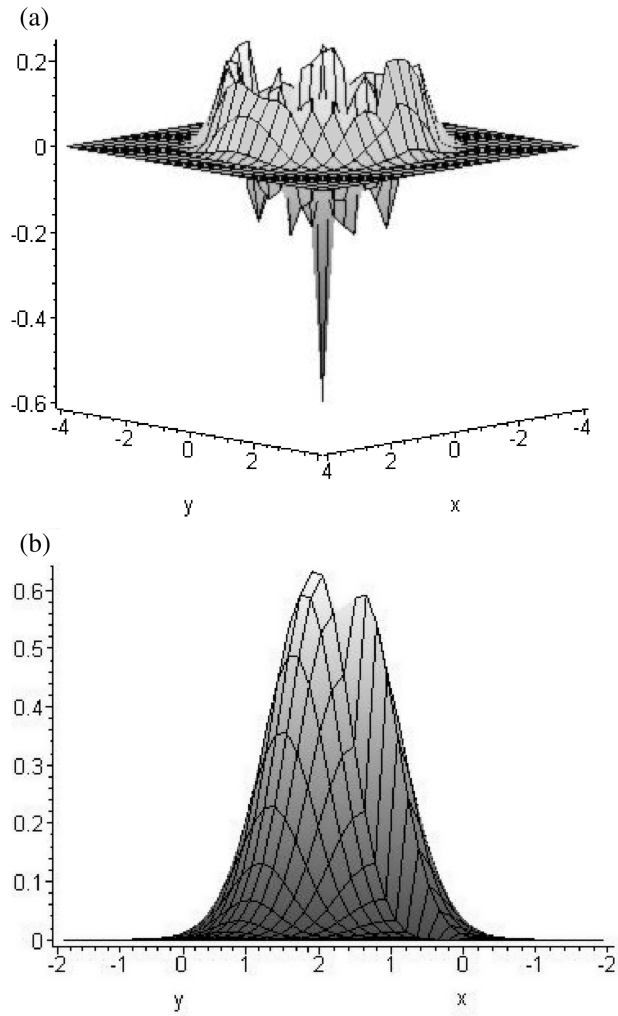

Figure 3. Plot of the Wigner function of the CCS, for $N = 5$ and (a) $\alpha = 0.4$; (b) $\alpha = 4$.

Wigner function indicate the state being nonclassical. Using the number-basis representation one can write, with $\tau = 1/2$ and $z = re^{i\theta}$, the Wigner function $R(z, 1/2) = W(r, \theta)$ in the form

$$W(r,\theta) = \frac{2\mathcal{N}'}{\pi} e^{-2r^2} \left\{ \sum_{n=0}^{N} (-1)^n n! |\alpha|^{2(N-n)} L_n(4r^2) + \sum_{n=0}^{N-1} \sum_{m=0}^{N} (-1)^n 2^{n-m+1} n! |\alpha|^{2N-n-m} r^{m-n} L_n^{m-n}(4r^2) \times \cos\left[\left(\gamma - \theta + \frac{\pi}{2}\right)(n-m)\right] \right\} \qquad (15)$$

where L_n^{m-n} are generalized Laguerre polynomials.

In figure 3(a) the Wigner function exhibits negative values whereas they are absent in figure 3(b). These results are in agreement with those of figure 2, which show the SP (super-Poissonian) effect when $\alpha = 0.4$ ($\alpha = 4$).

4.4. Nonclassical measure

Nonclassical effects exhibited by nonclassical states do not occur simultaneously. For example, squeezed-vacuum states show squeezing but are not SP whereas odd-coherent states are SP but show no squeezing. On the other hand, phase states are nonclassical but they show none of the traditional nonclassical effects (SP, anti-bunching, squeezing, interference in the phase space, etc). So, given two states exhibiting distinct nonclassical effects, asking 'which of them is more nonclassical than the other' is a pertinent question. The evaluation of the degree of nonclassicality of a state will be considered here for the CCS. Following [28] one defines the nonclassical measure of a state $|\Psi\rangle$ as the minimum of the distance between this state and the set of the most classical (coherent) ones, as follows:

$$d_m = \min_{\{|z\rangle\}} [1 - |\langle z|\Psi\rangle|^2] = 1 - \pi \max_{\{z \in C\}} Q_{|\Psi\rangle}(z) \qquad (16)$$

where $Q_{|\Psi\rangle}(z) = \langle z|\Psi\rangle\langle\Psi|z\rangle/\pi$ is the Husimi Q-function corresponding to the state $|\Psi\rangle$ and z is a complex variable associated with coherent states $|z\rangle$. The quantity d_m defined in equation (16) will be used to determine the nonclassical degree of the pure state $|\Psi\rangle$. It ranges from zero (most classical) to unity (most nonclassical). For Gaussian states, this measure is equivalent to the phase-space measure of nonclassicality [29, 30]. The Husimi Q-function for CCS can be obtained from equation (14) for $\tau = 1$. So, in the number-basis representation one can write, with $z = re^{i\theta}$, the Husimi Q-function $R(z, 1) = Q(r, \theta)$ in the form

$$Q_{|\mathrm{CCS}\rangle}(r,\theta) = \frac{\mathcal{N}'}{\pi} e^{-r^2} \left\{ \sum_{n=0}^{N} |\alpha|^{2(N-n)} r^{2n} + 2 \sum_{n=0}^{N-1} \sum_{m=0}^{N} |\alpha|^{2N-n-m} r^{m+n} \times \cos\left[\left(\gamma - \theta + \frac{\pi}{2}\right)(n-m)\right] \right\}. \qquad (17)$$

Substituting equation (17) in equation (16) we obtain the distance d_m in terms of the CCS parameters. We observe that, for $\alpha = 0.4$, d_m increases as N grows, ranging from 0.382

for $N = 1$, to 1 when $N \to \infty$ (not shown in the figures). Hence the CCS is always nonclassical and its nonclassical depth grows when the dimension N of the (truncated) Hilbert space increases. On the other hand, one observes that if α increases d_m decreases, so the state becomes more classical with growing values of α (not shown in the figures).

To avoid misunderstandings, we stress that one should distinguish between two Husimi Q-functions mentioned in this paper: one of them concerns that of the CCS, written in equation (17), allowing us to obtain the nonclassical degree d_m; the other, mentioned in the title of the paper, concerns that of arbitrary state $|\phi\rangle$, to be determined via the projection synthesis method [18], where the CCS just plays the role of an auxiliary state.

5. Comments and conclusion

In this paper we have employed the scheme of [16] to generate the CCS in travelling waves. This state is required in the projection synthesis scheme [19], for the experimental determination of the Husimi Q-function. The fidelity of the scheme is obtained by considering the noise introduced by nonideal photodetectors, which was accomplished through the Langevin operator method [22]. It was shown that, as a consequence of using nonideal photodetectors, the desired pure state to be generated emerges as a mixed state. Then the subsequent use of such a smeared state as auxiliary in the determination of the Q-function of another state will furnish a smeared Q-function. The application of the IBC allows one to recover the CCS from the smeared CCS. Reconstruction of the CCS allows one to recover the correct Q-function, as had been obtained from the ideal CCS. For the sake of completeness we have presented a brief study of some properties of the CCS, such as its photon number distribution (section 4.1), occurrence of SP statistics (section 4.2), its nonclassical depth (section 4.3), and its Wigner function (section 4.4).

Acknowledgments

We are indebted to Dr J Clausen for very enlightening discussions about the inverse Bernoulli convolution. We also thank the CNPq, FUNAPE(BB), and PRONEX(BB), Brazilian agencies, and VPG-UCG (NGA), for partially supporting this work.

References

[1] Vogel K, Akulin V M and Schleich W P 1993 *Phys. Rev. Lett.* **71** 1816
Parkins A S *et al* 1996 *Phys. Rev. Lett.* **71** 3095
[2] Brune M *et al* 1994 *Phys. Rev. Lett.* **72** 3339
[3] Davidovich L *et al* 1994 *Phys. Rev.* A **50** R895
[4] Pegg D T, Phillips L S and Barnett S M 1998 *Phys. Rev. Lett.* **81** 1604
[5] Guimarães Y A *et al* 2000 *Phys. Lett.* A **268** 260
[6] Villas-Boas C J *et al* 2001 *Phys. Rev.* A **63** 55801
[7] Meekhof D M *et al* 1996 *Phys. Rev. Lett.* **76** 1796
Meekhof D M *et al* 1996 *Science* **272** 1131
[8] Bennett C H *et al* 1993 *Phys. Rev. Lett.* **70** 1895
Bowmester C D *et al* 1997 *Nature* **390** 575
Julsgaard B *et al* 2001 *Nature* **413** 400
[9] Kane B E 1998 *Nature* **393** 143 and references therein
[10] Pellizzari T 1997 *Phys. Rev. Lett.* **79** 5242 and references therein
[11] Gisin N *et al* 2002 *Rev. Mod. Phys.* **74** 145
[12] see, e.g., Björk G and Sanchez-Soto L L 2001 *Phys. Rev. Lett.* **86** 4516
Mützel M *et al* 2002 *Phys. Rev. Lett.* **88** 083601 and references therein
[13] Zurek W H 1991 *Phys. Today* **44** 36
Gerry C C and Knight P L 1997 *Am. J. Phys.* **65** 964
Varcoe B T H *et al* 2000 *Nature* **403** 743
[14] Brune M *et al* 1990 *Phys. Rev. Lett.* **65** 976
Brune M *et al* 1992 *Phys. Rev.* A **45** 5193
[15] Yurke B and Stoler D 1986 *Phys. Rev. Lett.* **57** 13
[16] Dakna M *et al* 1999 *Phys. Rev.* A **59** 1658
[17] Gerry C C 1999 *Phys. Rev.* A **59** 4095
D'Ariano G M *et al* 2000 *Phys. Rev.* A **61** 053817
[18] Barnett S M and Pegg D T 1996 *Phys. Rev. Lett.* **76** 4148
[19] Baseia B, Moussa M H Y and Bagnato V S 1997 *Phys. Lett.* A **231** 331
[20] Moussa M H Y and Baseia B 1998 *Phys. Lett.* A **238** 223
[21] Valverde C *et al* 2003 *Phys. Lett.* A **315** 212
[22] Villas-Boas C J, de Almeida N G and Moussa M H Y 1999 *Phys. Rev.* A **60** 2759
[23] Kiss T, Herzog U and Leonhardt U 1995 *Phys. Rev.* A **52** 2433
[24] Dakna M *et al* 1998 *Acta Phys. Slov.* **48** 207
[25] Mandel L 1979 *Opt. Lett.* **4** 205
Short R and Mandel L 1983 *Phys. Rev. Lett.* **51** 384
Brattke S *et al* 2001 *Phys. Rev. Lett.* **86** 3535
Davidovich L 1996 *Rev. Mod. Phys.* **68** 127
[26] Dagenais M, Kimble H J and Mandel L 1977 *Phys. Rev. Lett.* **39** 691
[27] Glauber R J 1963 *Phys. Rev. Lett.* **10** 84
Sudarshan E C G 1963 *Phys. Rev. Lett.* **10** 277
[28] Malbouisson J M C and Baseia B 2003 *Phys. Scr.* **67** 93
[29] Lee C T 1991 *Phys. Rev.* A **44** R2775
[30] Lee C T 1995 *Phys. Rev.* A **52** 3374